Design of monopiles for multi-megawatt wind turbines at 50 m water depth

Njomo Wandji, Wilfried; Natarajan, Anand; Dimitrov, Nikolay Krasimirov; Buhl, Thomas

Published in:
European Wind Energy Association Annual Conference and Exhibition 2015, EWEA 2015 - Scientific Proceedings

Publication date:
2015

Document Version
Publisher's PDF, also known as Version of record

Design of monopiles for multi-megawatt wind turbines at 50 m water depth

Wilfried Njomo Wandji
DTU Wind Energy
wilw@dtu.dk

Anand Natarajan
DTU Wind Energy
anat@dtu.dk

Nikolay Dimitrov
DTU Wind Energy
nkdi@dtu.dk

Thomas Buhl
DTU Wind Energy
thbu@dtu.dk

Abstract:

The design of a monopile substructure for wind turbines of 10 MW capacity installed at 50 m water depth is presented. The design process starts with the design of a monopile at a moderate water depth of 26 m and is then up scaled to a 50 m water depth. The baseline geometry is then modified to specific frequency constraints for the support structure. The specific design requirements including the soil boundary conditions of this large diameter monopile has been described and fully coupled hydro-aero-servo elastic simulations are performed for ultimate limit state design. Soil plasticization is also considered. Analyses have shown that the design of large diameter monopile is not a straightforward extrapolation process, but it requires specific checks and iterations. An appropriate design scheme is proposed with perturbation analysis for robustness.

Keywords: Multi-megawatt wind turbines, large diameter monopile, deep water, ultimate design

1 Introduction

Offshore wind energy is moving towards larger turbines and into deeper waters. However, the wind energy industry is relatively recent and needs continuous improvements to its design practices. Two paths are used to improve wind energy productivity: reliability and more powerful wind turbines. The crossroads of these paths places the problem at the edges of the state of the art.

Indeed, wind turbines with rated capacity of 10 MW are being developed [1]. Their sizes necessitate suitable support structures that can withstand the engendered loads and last the intended life. Plus, their capacity needs enough wind resources to be fully exploited. This obliges that multi-megawatt turbines should be located in sites where wind resources are abundant. For this reason, recent potent sites have been found at deep waters (50+ m). They are able to provide enough wind resources as required by 10 MW wind turbines, but they also add to the challenge related to support structures.

Facing this challenge, space frame substructures have been proposed. However, their manufacturing process is daunting. In addition, there is a need to maintain the strength and stiffness requirements at the lowest possible cost [2]. In particular, a jacket structure has been proposed within the INNWIND.EU project [3] for a 10 MW turbine at 50 m water depths, but it has been extremely challenging to ensure jacket durability for 25 years with respect to its fatigue limit state. Besides the space frame solution, floating support structures are also a potential solution, but are economical at greater water depths over 100 m [2].

A monopile substructure solution at 50 m water depth is gaining more and more traction, due to the fact that its manufacturing process just consists of rolling and welding and its small footprint eases its transportation and its installation. This technology has been employed in many wind farms up to 30 m water depths composed usually of 2 to 5 MW wind turbines. For wind farms that combine larger wind turbines and deeper waters, significant design adaptation of the monopile is necessary to ensure structural integrity and cost effective manufacturing. Upscaling from present designs at lower water depths cannot be regarded as a straightforward process because of specific design requirements for large diameter monopiles.

The present paper proposes a preliminary design for large diameter monopiles at 50 m water depth. The study departs from current practices (middle size monopile) to accomplish its objectives. Precise design constraints are stated and large diameter monopile specifics are presented. Once a final

design is obtained, perturbation study is carried out, drawing additional conclusions.

2 Fully coupled aero-hydro-servo-elastic analysis

In addition to the controller, three media (air, sea, and soil) concurrently act on a given offshore wind turbine mounted on monopile. To ensure that all ambient interactions are adequately considered, a fully coupled design loads computation has been performed using the aero-hydro-servo-elastic software package HAWC2 [4].

HAWC2 utilizes a multibody formulation which couples different elastic bodies together. Bodies are composed of Timoshenko beam [5] finite elements whereby their stiffness, mass and damping are assembled into the governing equations of motion, whose solution is obtained using the Newmark-β method [6]. The damping coefficients are adjusted using Rayleigh coefficients to obtain desired damping ratios for the global structure. Blade Element Momentum (BEM) theory is employed for the rotor subjected to aerodynamics.

The turbulent wind field in the aeroelastic simulations is defined using the Mann model [7]. Tower shadow and aerodrag on all exposed elements are also accounted for. Random Gaussian 10-minute realizations are simulated over 11 mean wind speed bins between cut-in and cut-out wind speeds, and one mean wind speed related to the extreme load case. Each mean wind speed has been linked to a particular sea state.

The wave height is modeled based on a JONSWAP spectrum at the expected value of significant wave height and spectral peak period at each mean wind speed. Wave kinematics are computed according to the irregular Airy model with Wheeler stretching [8]. The hydrodynamic forces are computed based on the Morison equation [8] evaluated from water surface to seabed.

Below the seabed, soil-structure interaction is modeled as beam-on-nonlinear Winkler foundation with uncoupled responses of axial friction (t-z) and lateral force (p-y). American Petroleum Institute [9] recommends an algorithm to obtain p-y and t-z curves. Although [9] suggests using load-displacement behavior at unit tip, in the present study the nonlinear spring is replaced by a joint, restrained for vertical displacement and yaw rotation.

3 Site conditions, structure, and design constraints

In this study, the site conditions are taken from those described in [3]. The soil is made of superimposed sand layers of various properties each. The complete description of the adopted soil properties can be found in [3]. Above the soil, sea states are defined according to the atmospheric conditions (Table 1). Considering the JONSWAP wave spectrum, 95 % of the wave energy is realized under 0.225 Hz in the critical case. The off-resonance range related to wave excitation is hence restricted to above 0.225 Hz.

Table 1: Metocean conditions [3]

Wind speed [m/s]	Turbulence Intensity [%]	Significant height, Hs [m]	Peak period, Tp [s]
5	43.85	1.140	5.820
7	33.30	1.245	5.715
9	27.43	1.395	5.705
11	23.70	1.590	5.810
13	21.12	1.805	5.975
15	19.23	2.050	6.220
17	17.78	2.330	6.540
19	16.63	2.615	6.850
21	15.71	2.925	7.195
23	14.94	3.255	7.600
25	14.30	3.600	7.950
42.73	11.00	9.400	13.700

The DTU 10 MW reference wind turbine (DTU 10 MW RWT) [1] is used as mounted on a monopile substructure, whose design is sought. The tower is made of steel whose density is taken as 8500 kg/m^3 to account for the mass of secondary structures. Based on the rotor speeds, the corresponding Campbell diagram is drawn in Figure 1. This figure shows that 1P, 3P and 6P ranges are respectively in hertz [0.099, 0.158], [0.300, 0.480] and [0.600, 0.960].

The monopile is considered as made of hollow cylinder rolled from a steel plate of 7850 kg/m^3 whose characteristic strength is 500 MPa, which corresponds to high-strength steel. The monopile safety is assumed to be of component class 3. It can be fully defined by its outer diameter (D), wall thickness (t) and length. Its length consists of the part within the transition piece (26 m), the submerged part (50 m), and the embedded part below the soil level whose length is to be defined. The design of the monopile is carried out based on

the constructability and mass minimization. The following conflicting design aspects are analysed:

- larger outer diameter and smaller wall thickness lead to lighter piles and are easy to roll manufacture;
- larger outer diameter leads to large bending stiffness, but also to higher wave loads;
- smaller outer diameter leads to larger wall thickness and to deeper piles, but with reduced wave loading.

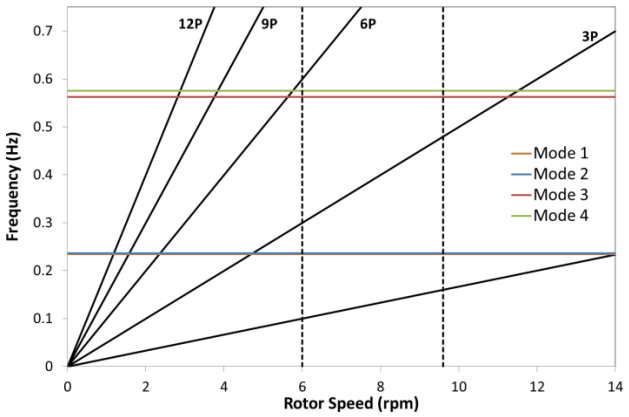

Figure 1: Campbell diagram

Practically, an upper limit of 10.00 m has been set for outer diameter in order to limit fluid-shaft interactions and to resort to large hammer. The selected wall thickness should withstand the stresses generated during pile-driving. In the absence of detailed analyses or past experiences, API (2005) [9] recommends that the minimum wall thickness should be taken as:

$$t\,[mm] = 6.35 + \frac{D\,[mm]}{100} \qquad (1)$$

In order to ease the rolling process, the wall thickness is restricted within the range [1, 1.1] times its recommended minimum value.

Besides the constructability and stability criteria, the monopile should also possess stiffness such that deformations are limited. In that respect, Krolis et al (2010) [10] have adopted a maximum displacement at the mudline of 120 mm and a maximum toe deflection of 20 mm. They found that these limitations can be fulfilled with embedded pile length between 5.3D and 4.4D for 3.0 MW turbines, and between 5.0D and 3.3D for 5.0 MW turbines.

In addition, the resulting design should provide enough dynamic stiffness such that the first frequencies of the overall structure lie between [0.225, 0.300] and [0.480, 0.600] in hertz. This requirement is important to minimize the fatigue effects generated by the vibrations, which are due to wind, wave, and rotor excitation during the structure lifetime.

4 Standard monopile at 26 m sea depth

The overall aim of this study is to determine the characteristic monopile properties so that the full structure has its first natural frequencies outside the resonance ranges. In order to achieve this target, the 10 MW wind turbine has been considered placed at a mean water depth of 26 m as a starting point. A corresponding monopile has been designed to fit the natural frequency requirements. As a first trial, a pile of 8.0 m outer-diameter and 100 mm wall thickness has been extruded from 26 m above mean water level till 50 m (= 6.25D) below the seabed i.e. a total of 102 m. The hub height above mean sea level is maintained at 119 m.

The steps required to tune the first natural frequencies outside resonance ranges are made by adjusting the wall thickness and the embedded depth of the monopile. From the initial design estimate, one parameter is varied and modal analysis is carried out with each of its value. The obtained natural frequencies are then checked against the admissible frequency range. Once a minimum satisfying value of the said parameter is obtained, it is set constant and another parameter is now varied till its minimum value that also satisfies the frequency requirement. This iterative process is repeated for all parameters.

Table 2: Wall thickness adjusting for 26 m sea depth

Wall thickness [mm]	Eigen frequencies [Hz]			
	Mode 1	Mode 2	Mode 3	Mode 4
90	0.224	0.227	0.544	0.584
100	0.229	0.232	0.545	0.584
120	**0.238**	**0.242**	**0.546**	**0.585**

The wall thickness has been fine-tuned to a value of about 120 mm as shown in Table 2 because the lower wall thickness cases of 100 mm and below provides a design too close to the resonance

frequency boundary. Further, considering this wall thickness, the embedded length has been adjusted. Table 3 shows that a satisfying value is 30 m.

Table 3: Embedded length below soil using a wall thickness t = 120 mm

Embedded length [m]	Eigen frequencies [Hz]			
	Mode 1	Mode 2	Mode 3	Mode 4
25.00	0.218	0.221	0.548	0.580
30.00	**0.227**	**0.230**	**0.548**	**0.587**
50.00	0.238	0.242	0.546	0.585

As a result of this process, a monopile of 8.0 m outer diameter, 120 mm wall thickness and 30 m embedded length satisfies the frequency requirement for the DTU 10 MW RWT placed at 26 m water depth.

5 Specificity of large diameter monopile

The model as described above works well for small to medium water depths but for greater depths, closer attention needs to be given to the structural stiffness distribution, influence of wave diffraction and soil-structure interaction.

For a given turbine moving from moderate to deep water, the longer cantilever length requires a wider monopile to provide enough stiffness to maintain the natural frequencies above that of wave excitation. However, it can be beneficial to distribute the added stiffness along the whole length by modifying the tower dimensions.

Furthermore, the wave diffraction phenomenon (for pile diameters greater than 20% of the wave length) for a vertical cylinder extending from the sea bottom through the free surface is proposed by MacCamy and Fuchs (1954) [11] as a correction for the inertia coefficient in the Morison equation at each metocean state.

Another factor to be taken into consideration is the soil-structure interactions wherein several issues are associated. For example, the p-y curve traditionally used has been developed for slender monopiles with up to approximately 2 m diameter ([12], [13]).

6 Geometry design

When placed at 50 m water depth, an initial monopile design estimate would be a cylinder with outer diameter of 10.0 m, wall thickness of 120 mm, and embedded length of 30 m, similar to what was achieved in the earlier design, but with a wider diameter. An iterative process similar to the one above is carried out.

Here, the outer diameter and the corresponding tower geometry are selected having in mind the necessary stiffness distribution along the structure height. This implies a thinner monopile but a wider tower. Table 4 shows adjustments of the outer diameter. In this table, diameter 10.0 m satisfies the resonance frequency requirements whereas diameter 9.5 m does not. Although the value of 9.5 m is found unsatisfactory in comparison to 10.0 m, the former is chosen and change is done on the tower geometry to compensate (Table 5). Table 6 shows that with the new tower, named B, there is a possibility to decrease monopile's wall thickness. Finally, a wall thickness of 110 mm is obtained. A value of 100 mm for wall thickness satisfies the frequency criterion but violates the minimum thickness as calculated by Eq. (1). The whole process as well as the obtained results is illustrated in Figure 2.

Table 4: Outer diameter adjustment with Tower A

Outer diameter [m]	Eigen frequencies [Hz]			
	Mode 1	Mode 2	Mode 3	Mode 4
9.50	**0.218**	**0.267**	**0.548**	**0.564**
10.00	0.225	0.227	0.549	0.565

Table 5: Tower selection

Tower type and mass [t]	Eigen frequencies [Hz]			
	Mode 1	Mode 2	Mode 3	Mode 4
A: 426.293	0.218	0.267	0.548	0.564
B: 511.131	**0.239**	**0.241**	**0.563**	**0.576**

Table 6: Wall thickness adjustment with Tower B

Wall thickness [mm]	Eigen frequencies [Hz]			
	Mode 1	Mode 2	Mode 3	Mode 4
110	**0.234**	**0.236**	**0.563**	**0.575**
120	0.239	0.241	0.563	0.576

By changing the tower from A to B, a global material save is made: from 3525.591 t to 3211.254 t. Plus, the rolling effort is preserved as wall thickness moves from 120 mm to 110 mm; the required driving power is made smaller; and the wave loads

have been decreased. For next paragraphs, outer diameter of 9.5 m, wall thickness of 110 mm, embedded length of 30 m and Tower B are considered.

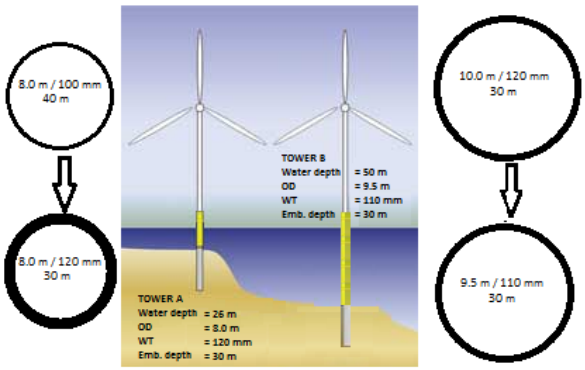

Figure 2: Design evolution

7 Characteristic curves

The global performance of the present design needs to be checked against that of the DTU 10 MW RWT. Generated power and aero rotor thrust as obtained from steady conditions are used as comparison criteria. The steady conditions are achieved by the application of steady wind whose speed linearly goes from cut-in to cut-out speed in 2500 s.

Figure 3 and Figure 4 respectively illustrate the curves of the generated power and of the aero rotor thrust plotted against the reference curves. These figures show that the present design performs as good as the reference as the curves almost superimpose each other.

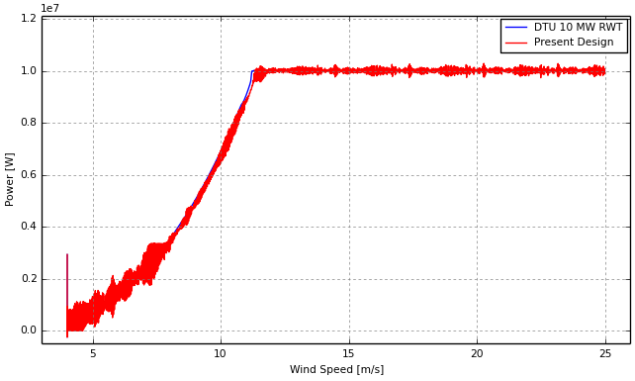

Figure 3: Power curve

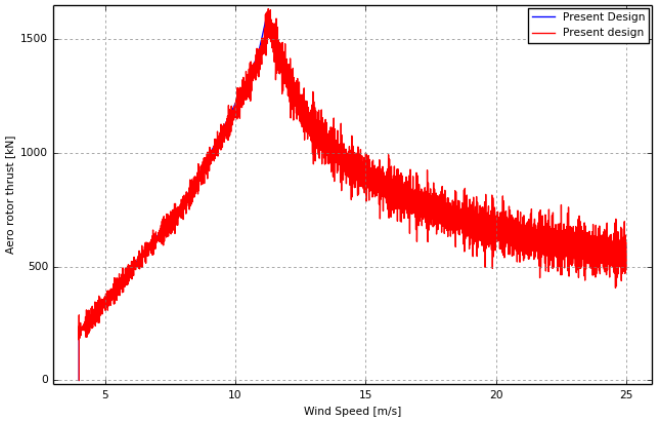

Figure 4: Aero rotor thrust curve

8 Ultimate limit state

8.1 Design load cases

The design at ultimate limit state has considered the model with articulated pile tip and shaft friction. Two load cases have been used here according to IEC 61400-3 [14]:

- DLC 1.3: six wind seeds for each of 11 wind speed bins have been applied each with no yaw error. Waves were aligned along wind direction. That makes 11 × 6 = 66 scenarios.
- DLC 6.2a: 42.73 m/s wind has been applied along 24 directions: from 0^0 to 345^0 in 15^0 steps. Waves were directed along wind direction with $\pm 30^0$ yaw error. With no active controller, the structure was loaded with an extreme current (1.2 m/s) of parabolic type at 0^0. Blades were pitched at 90^0 with no dynamic induction. This leads to a total of 24 × 3 = 72 scenarios.

8.2 Ultimate loads and deformation

Typical resultant shear force and bending moment curves are illustrated in Figure 5. In this figure, loads reach their maximum values in the embedded part. At about 7 m under the mudline, the moment value is maximal and the shear force is zero. At about 21 m depth in the soil, the monopile experiences maximal shear force. That location corresponds to zero-crossing point as it can be seen in Figure 6, which depicts a typical lateral displacement curve of the pile embedded portion. At that point, the monopile does not move laterally.

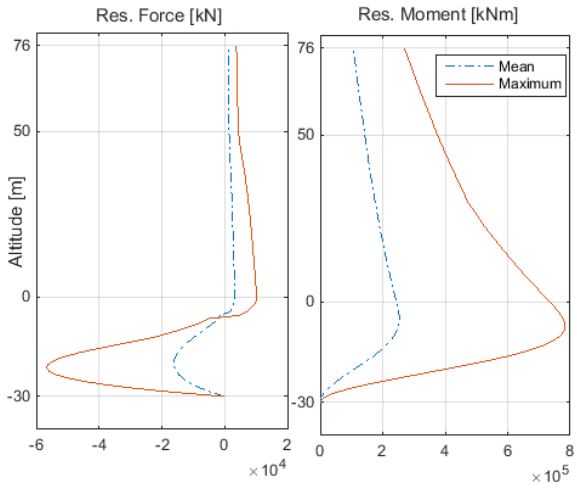

Figure 5: Typical resultant force and moment

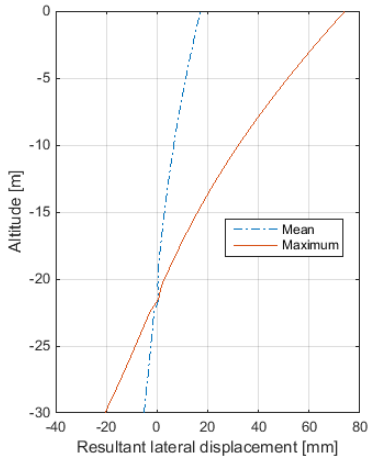

Figure 6: Typical lateral displacement

8.3 Stress check

Based on the internal forces and moments, maximum von Mises stresses are obtained for various sections along the pile portion going from mean water level to the tip. Three directional stresses have been combined according to the von Mises yield criterion: they are the axial stress, the circumferential stress, and the shear stress. Further details can be found in [15].

Figure 7 illustrates the design maximum von Mises stress distribution together with the steel design strength. The maximum design stress is about 251.9 MPa for a utilization factor of 72 %. This proves that the thickness is enough to withstand ultimate loads.

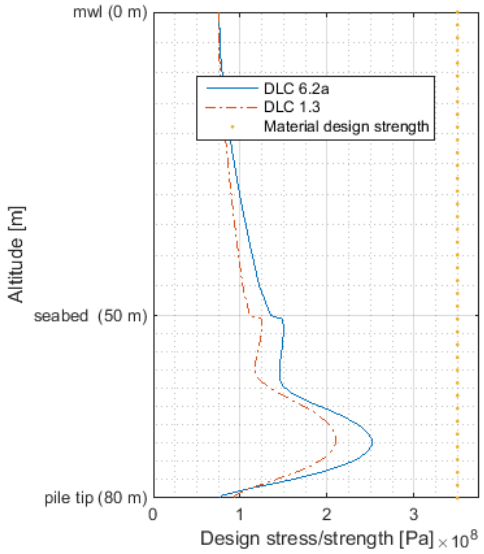

Figure 7: Design maximum von Mises Stresses

8.4 Deformation

The maximal displacement at the mudline is about 81 mm and the maximal tip deflection 22 mm. These values are globally acceptable with respect to the design constraints set above. However, as shown in Figure 8, the soil yield strength has been exceeded in approximately the first 10 meters from seabed. This value is intolerable as it represents one third of the foundation depth. The yielded zone shall be reduced. The perturbation analysis below investigates the possibilities for achieving this reduction.

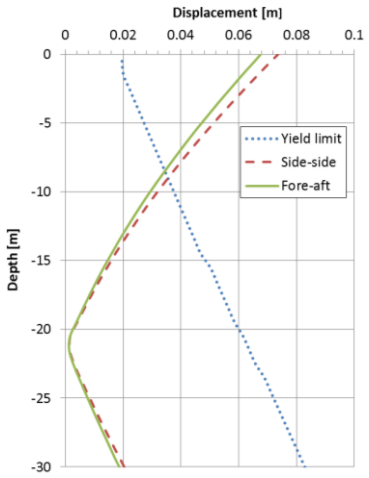

Figure 8: Elastic/Plastic zones

9 Investigation of perturbations

Holding the above design as baseline, five perturbation cases are considered for perturbation analysis. In addition to the baseline, the five other cases consist of:

- Baseline – The toe is modeled as a joint with restrained yaw and vertical motions. The contribution of the axial skin friction is accounted for. The monopile has a wall thickness of 110 mm, and is 26 m deep embedded into the soil whose internal friction angle is 35º.
- Perturbation A – Toe boundary condition. The pile tip is fixed, i.e. all degrees of freedom are restrained.
- Perturbation B – Axial skin friction contribution. The contribution of skin friction to the pile axial equilibrium has been annihilated.
- Perturbation C – Deeper pile. The embedded length of the pile has been changed from 30 m to 50 m.
- Perturbation D – Thicker wall. The wall thickness has been increased to 150 mm.
- Perturbation E – Soil friction angle. The soil around the pile is set denser; its internal angle has been improved from 35º to 38º.

The effects of each of these perturbations are investigated in terms of dynamic stiffness, deflections and yielded zone, and ultimate loads.

9.1 Dynamic stiffness

The dynamic stiffness is measured in terms of eigenfrequencies of the whole structure. As depicted in Figure 9, modal analysis results show that the respective modal frequencies are insignificantly different one from others. This observation reveals that none of the perturbation meaningfully influences the structure dynamic stiffness.

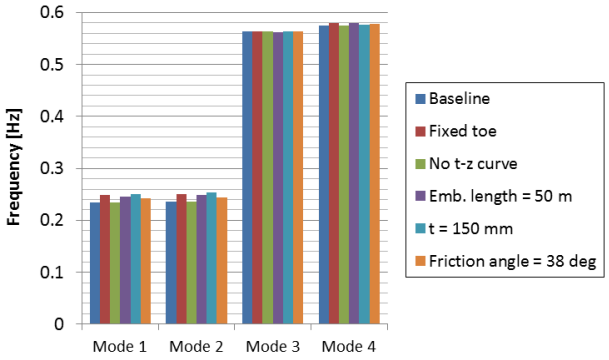

Figure 9: Modal frequencies for different perturbation

9.2 Deflection and plastic zone

However, Figure 10 shows some differentiation about the behavior of the perturbations regarding pile deflection. On the one hand, the skin friction contribution or the wall thickness increase does not bring any improvement. Their respective deformed shapes are similar to that of the baseline. On the other hand, fully fixing the toe or deepening the monopile leads to milder deformations (below 40 mm in each direction), and substantially reduces the yielded zone to about 5 m. On Figure 11, with the new internal friction angle, deformations have also decreased (between 40 and 60 mm in each direction). Considering the corresponding yield limit, the yielded zone is now about 7 m.

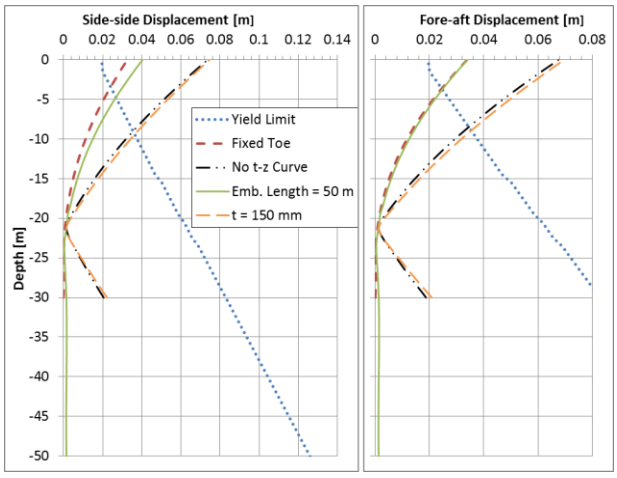

Figure 10: Deflection and yielded zones (Perturb. A, B, C, D)

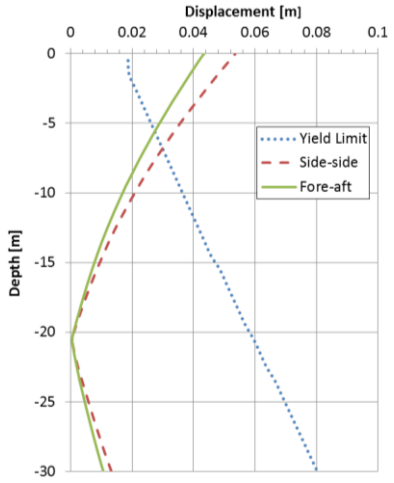

Figure 11: Deflection and yielded zones (Perturb. E)

9.3 Bill of material

Table 7 recapitulates the material mass used for each perturbation and for the baseline. It shows mass increase of 35.78% for the wall thickness change, and 18.87% for the length increase compared to the baseline mass. The other perturbations have the same mass as that of the baseline.

Table 7: Bill of quantities

Case	Baseline	A, B, E	C	D
Mass [t]	2700	2700	3210	3666
Rel. diff. [%]	-	0.00	18.87	35.78

9.4 Ultimate load

The maximum ultimate loads are given in Table 8 and in Table 9. They represent the load maxima obtained for each perturbation and for the baseline at the interface and at the mudline. They do not necessary occur simultaneously. It can be seen that these loads are respectively of the same ranges except the torsional moment from the deep pile case. This exceptional load value is more than twice the value of the other cases.

Table 8: Characteristic representative loads at interface – Deviation from the baseline

	Fres [kN]	Fz [kN]	Mres [kNm]	Mz [kNm]
Baseline	3500	13000	290000	-38000
Pert. A	0.0%	0.0%	3.4%	36.8%
Pert. B	0.0%	0.0%	0.0%	-234.2%
Pert. C	-2.9%	7.7%	-3.4%	-415.8%
Pert. D	-2.9%	0.0%	3.4%	-218.4%
Pert. E	2.9%	0.0%	3.4%	36.8%

Table 9: Characteristic representative loads at mudline – Deviation from the baseline

	Fres [kN]	Fz [kN]	Mres [kNm]	Mz [kNm]
Baseline	11000	40000	730000	-38000
Pert. A	0.0%	0.0%	2.7%	39.5%
Pert. B	9.1%	0.0%	0.0%	-236.8%
Pert. C	9.1%	0.0%	8.2%	-442.1%
Pert. D	0.0%	17.5%	2.7%	-221.1%
Pert. E	9.1%	0.0%	5.5%	39.5%

9.5 Discussion

Although all the cases (perturbations and baseline) have similar dynamic stiffness, they demonstrate different performance with respect to lateral deformations. This observation reveals that a design, exclusively based on dynamic stiffness, may be misleading. A thorough design process should continue till soil plasticization check as some perturbations have exhibited unchanged performance.

In particular, increasing the wall thickness does not bring any improvement. On the contrary, it introduces additional inconveniences. For example, it adds on to the total mass and requires more rolling effort. Consequently, the total cost will be increased. Similarly, shaft friction contribution happens to be non-influential. This may be due to the fact that the vertical degree of freedom has been restrained. Further investigations on axial skin friction may be carried out with a pile tip unrestrained in all directions.

Fixing all toe degrees of freedom produces a positive effect. However, the monopile toe is factually fixed if it is rooted into a rock, for example. If this is not the actual circumstance, this modeling approach may lead to misrepresentative results. In this case, results show that the best solution is to lengthen the monopile. Deepening the monopile increases the mass to some extend but significantly enhances the design. However, a drawback is the increase of torsional moment in the structure. It is expected that the account for the soil torsional resistance (M-θ curve) can contribute to mitigate this shortcoming.

10 Conclusion

In conclusion, the design of monopile for multi-megawatt wind turbines at 50 m water depth is carried out. The process started with the design of a monopile at 26 m water depth. Then, its upscaling

has served as baseline geometry for 50 m water depth. The specificity of large diameter monopile has been stated and implemented. Analyses have shown that (i) the initial tower was not apposite for the design constraints; and (ii) a large amount of soil got plasticized.

With a new tower, five perturbation cases have been considered. Their examinations reveal that a design exclusively based on avoiding resonant frequency may not be thorough. An appropriate design scheme for large diameter monopile, however, could be extracted from the assessments. Indeed, the geometry that satisfies the resonant frequency range criterion is a good starting point. Attention should be taken to distribute the stiffness along the structure: a change of the tower properties can be necessary. The design is completed by setting a sufficient length that gives desired deflection shape.

Updating the pile length leads to increase of torsional moment. Further studies need to investigate how the consideration of soil torsional resistance can affect this observation. In addition, accounting for tip-displacement relationship might also reveal salient conclusions, namely about the influence of the skin friction. Finally, more detailed soil-structure interaction can also be regarded. This includes coupled load-displacement relationships, gapping phenomena and cyclic behavior.

Acknowledgements

The research leading to these results has received funding from the European Community's 7th Framework Programme FP7-ENERGY-2012-1-2STAGE under grant agreement No. 308974 (INNWIND.EU) and also from the Danish Energy Agency EUDP project titled, "Offshore wind turbine reliability through complete loads measurements", project no. 64010-0123. The financial support is greatly appreciated.

References

[1] Bak C, Zahle F, Bitsche R, Kim T, Yde A, Henriksen LC, Andersen PB, Natarajan A, Hansen MH. "Design and performance of a 10 MW wind turbine". http://www.innwind.eu/-/media/Sites/innwind/Publications/Deliverables/DeliverableD1,-d-,21ReferenceWindTurbinereport_INNWIND,-d-,EU.ashx?la=da

[2] Jonkman JM, Buhl Jr ML. "Loads analysis of a floating offshore wind turbine using fully coupled simulation". WindPower 2007 Conference & Exhibition Los Angeles, California, June 3–6, 2007.

[3] Von Borstel T. "INNWIND Design Report Reference Jacket", Ramboll. 2013. http://www.innwind.eu/-/media/Sites/innwind/Publications/Deliverables/DeliverableD4,-d-,31_20131030_INNWIND,-d-,EU.ashx?la=da

[4] Larsen TJ, Hansen AM. How 2 HAWC2, the user's manual. DTU Wind Energy: Risoe, 2014.

[5] Przemieniecki JS. Theory of matrix structural analysis. McGraw-Hill, 1968.

[6] Chopra AK. Dynamics of structures. Prentice-Hall: Upper Saddle River, N.J., 2011.

[7] Mann J. "The spatial structure of neutral atmospheric surface-layer turbulence". Journal of Fluid Mechanics 1994; 273:141–168.

[8] Chakrabarti SK. Handbook of Offshore engineering. Elsevier: Oxford, 2005, Vol. 1.

[9] American Petroleum Institute. Recommended practice for planning, designing and constructing fixed offshore platforms—Working stress design. API RP 2A-WSD, 2005.

[10] Krolis VD, van der Zwaag GL, de Vries W. "Determining the embedded pile length for large-diameter monopiles". Marine Technology Society Journal 2010; 44(1): 24-31.

[11] MacCamy RC, Fuchs RA. Wave forces on piles: A diffraction theory. Corps of Engineers 1954.

[12] Pradhan DL. Development of P-Y Curves for Monopiles in Clay using Finite Element Model Plaxis 3D Foundation. Master Thesis NTNU 2012.

[13] Bekken L. Lateral behaviour of large diameter offshore monopile foundations for wind turbines. TU Delft Master Thesis 2009.

[14] The international Electrotechnical Commission: Wind Turbines – Part 3: Design requirements for offshore wind turbines, IEC 61400-3 Ed 1, 2009.

[15] Koukoura C. Validated loads prediction models for offshore wind turbines for enhanced component reliability. DTU PhD Thesis 2014.